

# Second harmonic generation investigations of charge transfer at chemically-modified semiconductor interfaces

Vasiliy Fomenko, Cédric Hurth, Tao Ye, and Eric Borguet<sup>a)</sup>

*Department of Chemistry and Surface Science Center, University of Pittsburgh, Pittsburgh, Pennsylvania 15260*

(Received 3 October 2001; accepted for publication 18 December 2001)

Charge transfer and accumulation at semiconductor devices can lead to device degradation. Understanding and controlling such a process is therefore important. Second harmonic generation has been shown to be a sensitive probe of charging of semiconductor interfaces, with the added advantages of high spatial and temporal resolution. We have investigated the use of self assembled monolayers (SAMs) as a means to control charging. Our results suggest that octadecylsiloxane SAMs, bound to the native oxide, significantly reduce charge accumulation at oxide interfaces. © 2002 American Institute of Physics. [DOI: 10.1063/1.1452774]

## I. INTRODUCTION

Charge transfer, trapping, and detrapping were recently reported by Mihaychuk *et al.* to induce transient, i.e., time-dependent second harmonic generation (TD-SHG) response from oxidized Si(100) irradiated by a fsec Ti:sapphire oscillator.<sup>1</sup> The *p*-in/*p*-out SHG response grew to a saturation value on a time scale of seconds, faster at higher incident laser intensity. Similar effects were reported for the *s*-in/*p*-out polarization combination,<sup>2</sup> for various oxide thicknesses,<sup>3</sup> doping levels and doping types for Si(100)<sup>1–6</sup> and for fundamental wavelengths in the range of 710–800 nm.<sup>4</sup> TD SHG was also observed for oxidized Si(111)<sup>2</sup> and for intrinsic Si.<sup>1</sup> SHG signals recovered from the saturation level if the sample was held in the dark for a few minutes.<sup>1</sup> Mihaychuk *et al.* ascribed TD-SHG to charge transfer across the Si–SiO<sub>2</sub> interface, and trapping leading to a variation in the interfacial charge and a change in the nonlinear susceptibility.<sup>1,3,4</sup> The rise time of the signal is determined by the rate of trapping and detrapping, while the rate of the decay/dark recovery is related to detrapping alone.<sup>1</sup> The magnitude of the induced signal is related to the magnitude of the trapped charge at the interface. The value of the trapping time constants showed a nonlinear dependence on laser fluence, suggesting a multiphoton-mediated process.<sup>1</sup>

While the influence of the ambient environment on the TD SHG has also been investigated, the role of the chemical nature of the interface and how charge trapping might be controlled by chemical means is less well understood.<sup>2,7,8</sup> Organic molecules, due to their low electric conductivity and the possibility of forming layers of monolayer thickness are considered as useful candidates for building thin insulating layers at interfaces.<sup>9</sup> Organic monolayers are also promising for the development of molecular electronics.<sup>9,10</sup> Recently, the use of organic molecules (long-chain hydrocarbons) to control charge transfer in metal–insulator–semiconductor structures has been reported.<sup>10,11</sup> Densely-packed, self-

assembled monolayers (SAMs) of hydrocarbons were shown to reduce carrier tunneling by 4–5 orders of magnitude compared to silicon dioxide of similar thickness.<sup>10,11</sup>

SHG is a versatile probe of buried semiconductor interfaces.<sup>12</sup> Time-dependent SHG has enabled the temporal evolution of interface charging to be followed as carriers are promoted across the Si/SiO<sub>2</sub> interface.<sup>1,4,6</sup> The trapped interfacial charge induces an electric field  $E_{DC}$  in the near-interface region, resulting in an electric-field-induced second harmonic (EFISH) source term that adds to the usual  $\chi^{(2)}$  term:

$$I(2\omega) = C|\chi^{(2)} + \chi^{(3)}:E_{DC}|^2 I^2(\omega). \quad (1)$$

$E_{DC}$ , the interfacial field, depends implicitly on time due to interfacial charge transfer and  $\chi^{(3)}$  is a third-order susceptibility that generates the electric-field driven, bulk dipole response.<sup>3</sup> The presence of ambient gases, in particular oxygen, has been shown to increase the charge buildup through capture of electrons in a “harpooning reaction<sup>3</sup>”.

Our objective was to explore the possibility of eliminating ambient atmospheric effects on the laser-induced charge transfer, and to better separate the possible mechanisms contributing to the charging/discharging process and the role of different possible traps. To this end, TD-SHG experiments were performed on chemically-modified Si interfaces. We provide evidence that the presence of a SAM on oxide-covered Si(111) samples significantly reduces charge transfer behavior and associated TD SHG effects.

## II. EXPERIMENT

The SHG experiments were performed with a sub-100-fs, 76 MHz Ti:sapphire oscillator (coherent Mira Seed), pumped with all lines of an Ar<sup>+</sup> ion laser (Coherent Innova 310). Equipped with a birefringent filter and custom optics, the laser was tunable from 720 to 930 nm. Light was focused at 45° with respect to the surface normal by a 100 mm lens, ( $f\# = 32$ ). The focused-spot diameter, measured by the knife-edge technique, was  $32 \pm 2 \mu\text{m}$  ( $1/e^2$  criterion) in good agreement with the value of  $32 \mu\text{m}$  calculated for a

<sup>a)</sup> Author to whom correspondence should be addressed; electronic mail: borguet@pitt.edu

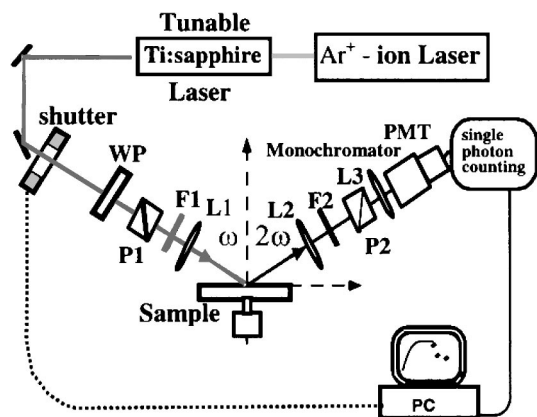


FIG. 1. Time-dependent second harmonic generation experimental setup: (WP)- $\lambda/2$  waveplate; (P1)-input polarizer; (F1) red filter, (L1)-focusing lens, (L2)-collimating lens, (F2)-blue filter (aqueous solution of  $\text{CuSO}_4$ ), (P2)-UV polarizer, and (L3)-focusing lens.

diffraction-limited spot of a perfect Gaussian beam. The laser input power was varied with a ( $\lambda/2$  waveplate)–polarizer combination under computer control. SHG signals were detected by the single-photon counting technique after appropriate spectral filtering using a filter/monochromator/red-blind photomultiplier tube combination, Fig.1.

The polarization of the incident fundamental and the reflected second harmonic light were analyzed by polarizers (Tower Optics Corp. and Karl Lambrecht Corp.) whose extinction coefficient was better than  $5 \times 10^{-5}$ . All scans were taken at 730 nm  $p$ -polarized input light and  $p$ -polarized SH intensity was recorded unless otherwise indicated. The samples were azimuthally oriented to a maximum of the rotational anisotropy pattern, as determined at low power, unless otherwise indicated.

Experiments were performed on Czochralski-grown  $n$ -type, phosphorus-doped ( $>50 \Omega \text{ cm}$ ), Si(111) samples (Silicon Quest),  $\approx 0.5 \text{ mm}$  thick and polished on both sides. “Native oxide” refers to polished samples used as received, degreased by sonicating in trichloroethylene (J.T. Baker, “Baker analyzed” reagent grade), then methanol (Fisher Scientific, reagent grade), then acetone (EM Science, “guaranteed reagent” grade), for 10 min. each. The chemicals for sample treatment were used as received. The oxide thickness was measured by ellipsometry to be  $1.8 \pm 0.1 \text{ nm}$  for Si(111)/ $\text{SiO}_2$  after degreasing. The refractive indices were taken to be  $n_{\text{Si}} = 3.882$ ,  $k_{\text{Si}} = 0.019$  for Si,<sup>13</sup>  $n_{\text{SiO}_2} = 1.46$  for  $\text{SiO}_2$ <sup>13</sup> and,  $n_{\text{ODS}} = 1.45$  for ODS,<sup>14</sup> at 638.2 nm. Ellipsometric measurements were carried out on a Gaertner Scientific null ellipsometer (model L117) at 632.8 nm and at  $70^\circ$  angle of incidence.

Prior to SAM preparation, the Si(111) wafers were cleaned in an SC1 mixture  $\text{H}_2\text{O}_2$  (CMOS grade, J.T. Baker):  $\text{NH}_4\text{OH}$  (EM Science, “guaranteed reagent” grade):  $\text{H}_2\text{O}$  ( $>18 \text{ M}\Omega \text{ cm}$ ), (1:1:4) volume ratio for 30 min at  $80^\circ \text{C}$ , followed by rinsing the sample in ultrapure water ( $>18 \text{ M}\Omega \text{ cm}$ ). The sample was then irradiated by a low-pressure Hg/Ar (intensity  $\sim \text{mW/cm}^2$ ) ultraviolet (UV) lamp

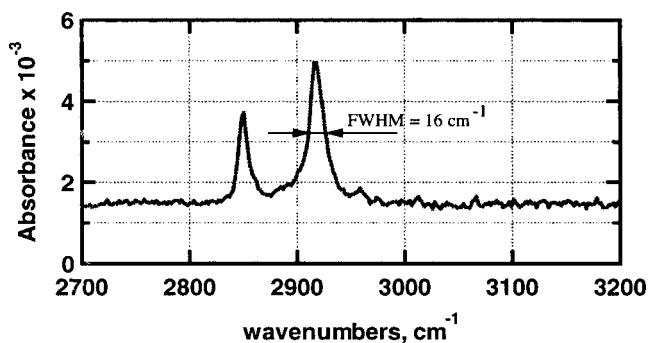


FIG. 2. Normal-incidence transmission FTIR spectrum of the Si(111)/ $\text{SiO}_2$ /ODS surface.

(Oriol Instruments), emitting principally 184 and 254 nm for 2 h in ambient laboratory air. This results in photodegradation of organic contaminants by combined action of UV photons and reactive oxygen species.<sup>15</sup> Such treatment led to a slight increase in the oxide thickness to  $2.1 \pm 0.1 \text{ nm}$  as measured by ellipsometry.

An octadecylsiloxane (ODS) SAM was prepared on oxidized silicon substrates by immersion in 2.5 mM octadecyltrichlorosilane (Acros, 95%) solutions prepared in a mixture of hexadecane (Acros, 99%):  $\text{CHCl}_3$  (EM Science, “guaranteed reagent” grade):  $\text{CHCl}_4$  (Aldrich, 99%), 10:1:1.5 volume ratio.<sup>16</sup> The preparation of the SAM was carried out at  $23^\circ \text{C}$ , with the relative humidity of the ambient air maintained at 50%. Both the humidity and the temperature play a crucial role in ODS SAM formation.<sup>17,18</sup> First, it is important for successful SAM preparation that the substrate surface be hydrated with a nanometer-thin layer of water.<sup>17</sup> The 50% humidity was reported as optimal for dense horizontal polymerization of trichlorosilanes, and formation of a compact SAM.<sup>19</sup> Second, the deposition temperature should be maintained below a critical value  $T_c$  that depends on chain length and is equal to  $28^\circ \text{C}$  for ODS.<sup>18</sup> The thickness of the alkylsiloxane monolayer on the top of the oxide was estimated by ellipsometry to be  $2.9 \pm 0.1 \text{ nm}$  in good agreement with the value of 2.6 nm estimated by the formula  $d(C_n) = 0.126(n-1) + 0.478 \text{ nm}$  valid for hydrocarbons oriented perpendicularly to the solid substrate and extended in their all-trans conformation.<sup>10,20</sup> The difference of 0.3 nm could be associated with the terminal Si–O groups of the alkylsiloxane attached to the surface of  $\text{SiO}_2$ . The measured thickness is consistent with a nearly vertical orientation of the alkyl-chains, in agreement with a literature report of a tilt angle of  $10^\circ$ .<sup>17</sup>

Water and hexadecane contact angles were measured with a VCA-2000 contact angle apparatus on a horizontally-oriented sample surface. A normal-incidence transmission Fourier transform infrared (FTIR) (Nicolet Avatar 360) spectrum of the double-sided ODS-covered sample, (Fig.2) was acquired in dry air atmosphere at  $4 \text{ cm}^{-1}$  resolution by averaging 256 scans with a clean Si/ $\text{SiO}_2$  wafer as a background.

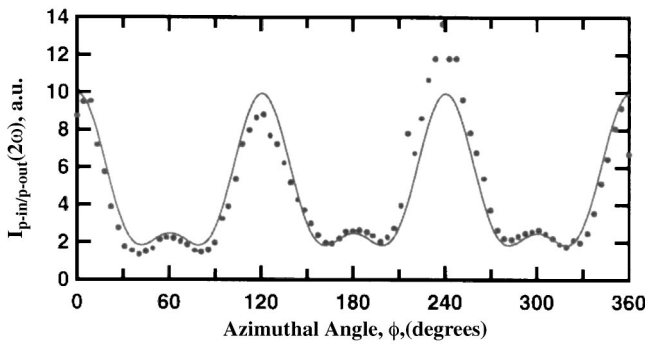


FIG. 3. Second harmonic generation rotational anisotropy response of *n*-Si(111)SiO<sub>2</sub> interface in *p*-in/*p*-out polarization combination and 10kW/cm<sup>2</sup> average irradiance,  $\phi=0$  is along the  $[2\ \bar{1}\ \bar{1}]$  direction.

### III. RESULTS AND DISCUSSION

#### A. TD SHG from natively oxidized Si(111)

Prior to TD-SHG experiments, a SHG rotational anisotropy pattern from Si/SiO<sub>2</sub> was recorded, Fig. 3. Time dependent SHG experiments were carried out by monitoring the SHG response of the sample as a function of Ti:sapphire oscillator illumination time counting photons continuously in 0.5 s intervals, until SHG approached saturation. Then, the laser was blocked. The recovery of the SHG response was followed by unblocking the laser periodically and sampling the SHG for ~ 1 s. At 730 nm, [Fig.4(a)], the SHG signal rise to saturation occurs on a time scale of hundreds of seconds. The recovery of the SHG signal is slower. The somewhat shorter saturation times reported for intrinsic Si(100) are probably related to a different initial carrier density, shown to affect charging/accumulation times.<sup>1</sup> The initial carrier density is important since it determines both the integral value of the screened electric field in the material and the TD-SHG time constants.<sup>4</sup> The excitation wavelength was chosen to be 730 nm because the SH wavelength (365 nm, 3.4 eV) is resonant with the *E*<sub>1</sub> direct energy gap of Si, Fig. 5.<sup>4,21,22</sup>

TD-SHG has been ascribed to EFISH associated with charge transfer at the SiO<sub>2</sub> interface.<sup>1,4</sup> To reach the SiO<sub>2</sub>-ambient interface, electrons first need to populate the SiO<sub>2</sub> conduction band, presumably through three-photon absorption.<sup>4</sup> When the SH is resonant with a critical-point transition, e.g., the *E*<sub>1</sub> point, promotion of carriers to the oxide conduction band may be resonantly enhanced through two-photon excitation to the substrate conduction band and then, by subsequent one-photon absorption, to the oxide conduction band.<sup>23</sup> Photoexcited carriers may be trapped in three different regions of the sample:<sup>24</sup>

- (i) at the semiconductor/oxide interface;
- (ii) in the SiO<sub>2</sub> bulk; and
- (iii) at the SiO<sub>2</sub> ambient interface.

Trapping of electrons at the SiO<sub>2</sub> ambient interface can be enhanced by adsorption of ambient gases, in particular, oxygen.<sup>3</sup>

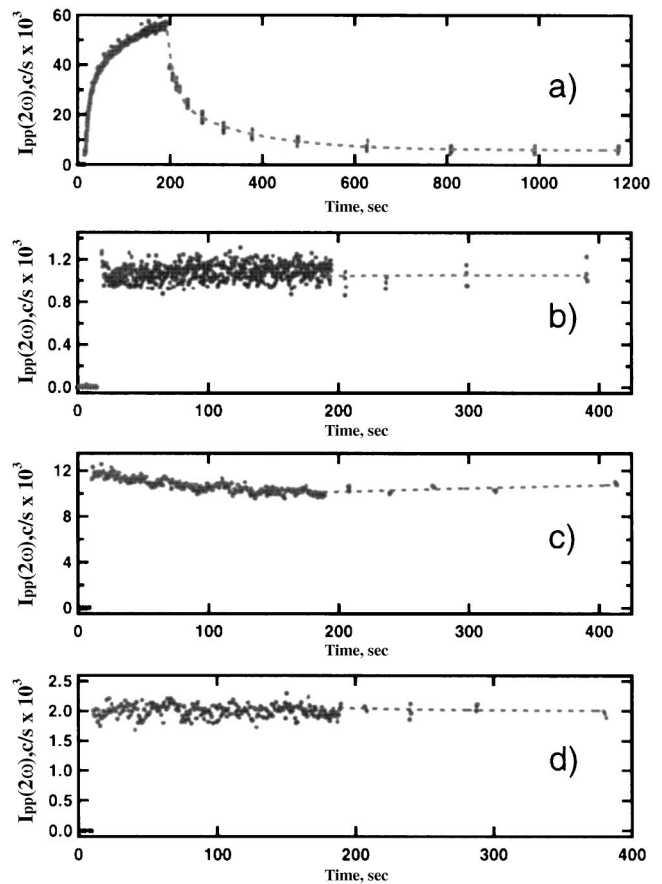


FIG. 4. TD-SHG (365 nm) response of Si(111) interfaces in *p*-in/*p*-out polarization combination and 10kW/cm<sup>2</sup> average irradiance. Dashed line drawn to guide the eye: (a) *n*-Si(111)/SiO<sub>2</sub> at a **major maximum** of the rotational anisotropy pattern ( $\phi=0$ ). isotropic and anisotropic contributions to TD SHG are in phase; (b) *n*-Si(111)/SiO<sub>2</sub> at a **minor maximum** ( $\phi=60^\circ$ ) of the rotational anisotropy pattern. anisotropic and isotropic contributions to TD SHG are out of phase; (c) *n*-Si(111)/SiO<sub>2</sub>/ODS interface at the maximum of the rotational anisotropy pattern; and (d) *n*-Si(111)SiO<sub>2</sub>/ODS interface, **60° away from the maximum** of the *p*-in/*p*-out rotational anisotropy pattern.

#### B. Azimuthal dependence of TD SHG

The TD-SHG behavior depends on sample azimuth. The TD SHG at an azimuth shifted 60° from a maximum peak of the rotational anisotropy shows almost no transient response,

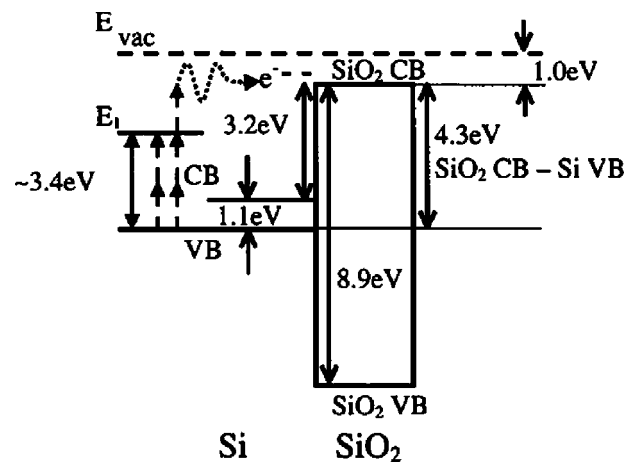


FIG. 5. Energy diagram for Si-SiO<sub>2</sub> and paths of charge transfer. See Refs. 4 and 21.

Fig. 4(b). This can be understood by considering the anisotropy of the nonlinear response resulting from the anisotropy of the  $\chi^{(3)}$  tensor. The bulk-dipole-governed, electric-field-induced contribution  $P_{2\omega}^{\text{BD}}(E_{\text{DC}})$  to *p*-in/*p*-out SHG response, for the (111) surface of a cubic crystal, is given by the following expression:<sup>25</sup>

$$P_{2\omega}^{\text{BD}}(E_{\text{DC}}) = a^{\text{BD}}(E_{\text{DC}}) + b^{\text{BD}}(E_{\text{DC}})\cos(3\phi). \quad (2)$$

The azimuthal angle  $\phi$  is measured between the plane of incidence and the  $[2\ 1\ 1]$  direction.<sup>26</sup> Since  $E_{\text{DC}}$  results from charge accumulation at the interface, which depends on the duration and nature of the irradiation, the EFISH contribution becomes time dependent.

Equation (2), has isotropic and anisotropic contributions.<sup>25</sup> Comparing the TD SHG at  $\phi=0^\circ$ , Fig. 4(a), and at  $\phi=60^\circ$ , Fig. 4(b), one can estimate the relative magnitude and phase of the isotropic and anisotropic contributions. Differences in the relative increase of TD SHG at these azimuths reflect differences in the magnitudes and phase of the isotropic and anisotropic parts of the  $\chi^{(3)}$  tensor. For the TD-SHG signals, measured at a major maximum ( $\phi=0^\circ$ ) and minor maximum ( $\phi=60^\circ$ ) of the rotational anisotropy, one can show

$$\begin{aligned} \frac{\Delta I_{\phi=60}}{\Delta I_{\phi=0}} &= \frac{|P_{2\omega}^{\text{BD}}|_{\phi=60}^2}{|P_{2\omega}^{\text{BD}}|_{\phi=0}^2} = \frac{|a^{\text{BD}}(E_{\text{DC}}) - b^{\text{BD}}(E_{\text{DC}})|^2}{|a^{\text{BD}}(E_{\text{DC}}) + b^{\text{BD}}(E_{\text{DC}})|^2} \\ &\approx 0 \Rightarrow \frac{|b^{\text{BD}}|}{|a^{\text{BD}}|} \approx 1, \end{aligned} \quad (3)$$

where  $\Delta I(2\omega)$  is the increase in SHG upon irradiation.

The isotropic and anisotropic components of  $\chi^{(3)}$  contribute in phase at  $\phi=0^\circ$ , Fig. 4(a), and out-of-phase at  $\phi=60^\circ$ , Fig. 4(b), to the TD SHG. Therefore, one can conclude that  $a^{\text{BD}}$  and  $b^{\text{BD}}$  are in phase and are similar in magnitude. Furthermore, the data suggest that both  $a^{\text{BD}}(E_{\text{DC}})$  and  $b^{\text{BD}}(E_{\text{DC}})$  increase as a result of interface charging.

At  $\phi=0^\circ$ , the SHG signal on a previously unirradiated region of the Si-SiO<sub>2</sub> sample was found to be nonquadratic. The power dependence was quadratic on a freshly irradiated region. Non quadratic behavior recovered if the sample was left in the dark for several minutes. Quadratic behavior was always observed at  $\phi=60^\circ$ , in the power range explored. This behavior is not a result of photoinduced carrier screening of the electric field in the space-charge region of the semiconductor sample.<sup>23,27</sup> The power density employed here is too large to observe the effects reported in Ref. 27. Rather, the nonquadratic behavior on unirradiated regions is a cumulative effect of laser induced charge trapping during the SHG measurements. Once a region is charged, quadratic behavior prevails as long as the laser does not further perturb the sample or significant trapped charge depletion occurs. The azimuthal dependence of the nonquadratic behavior is consistent with charge induced EFISH adding to the intrinsic second order response of the system.

### C. TD-SHG from SAM-covered Si(111)/SiO<sub>2</sub>

Alkylsiloxane SAMs have been frequently employed to change the surface properties of oxides since the early work

of Sagiv.<sup>16</sup> ODS reacts with the SiO<sub>2</sub> layer to form a SAM of octadecylsiloxane chains by covalent attachment to the surface Si-OH groups.<sup>10,14</sup> The ODS alkyl chains render the surface hydrophobic.

The presence of an ODS monolayer should render trapping at the oxide/ambient interface inactive by providing an impenetrable barrier to gas diffusion to the oxide/SAM interface. The experimental results appear to bear out this hypothesis. While laser irradiation of the Si/SiO<sub>2</sub>/ODS samples does lead to some TD SHG, the amplitude of change in the SHG intensity is significantly smaller, by a factor of 30, than in the case of the Si/SiO<sub>2</sub>/ambient, [Fig. 4(c)]. The SHG signal changes less than 20% from its initial value as compared to the order of magnitude increase observed for Si/SiO<sub>2</sub>/ambient systems, [Fig. 4(a)]. It should be noted that the SHG on ODS-covered Si/SiO<sub>2</sub> recorded at an azimuth, which is 60° off the maximum of the rotational anisotropy pattern, also shows no time-dependent behavior, [Fig. 4(d)]. Our hypothesis is that the presence of a SAM prevents or retards ambient gases, particularly oxygen, from adsorbing to the SiO<sub>2</sub>/ambient-air interface because the gas cannot diffuse easily to the SiO<sub>2</sub> surface through the long carbon chains of the compact ODS SAM. In addition, the ODS monolayer serves as a barrier to keep hot electrons from reaching the ambient interface due to excellent insulating properties of the SAM.<sup>10,11</sup> Therefore, the capture of electrons by adsorbed oxygen is significantly attenuated at the ambient interface. The much smaller time dependence of SHG when ODS is incorporated onto the oxide/ambient interface, is consistent with blocking of this possible trap region.

Residual time dependence of SHG, [Fig. 4(c)], can result from a number of different effects. It may, for example, reveal incomplete blocking of the oxide interface by the SAM due to pinholes or disorder in the monolayer or the influence of other traps, e.g., those at the Si-SiO<sub>2</sub> interface or in the bulk oxide. However, the FTIR spectrum, (Fig. 2), suggests that the monolayer is highly ordered based on the peak positions, peak full-width half maxima (FWHM), and absorbance of the CH<sub>2</sub> stretch peaks.<sup>28-30</sup> The peak positions of the CH<sub>2</sub> symmetric (2849 cm<sup>-1</sup>) and the CH<sub>2</sub> asymmetric (2918 cm<sup>-1</sup>) vibrations, as well as the magnitude of the CH<sub>2</sub> asymmetric-stretch-peak absorbance, 3.5 mOD, (Fig. 2), correspond to values reported for densely packed full monolayers.<sup>28-30</sup> The FWHM of the CH<sub>2</sub> asymmetric stretch peak, 16 cm<sup>-1</sup>, is also in good agreement with the value of 17 cm<sup>-1</sup> reported for full-monolayer, densely packed ODS on silica in transmission FTIR.<sup>28</sup> The FTIR results are further corroborated by the high contact angles of water (111°±1°) and hexadecane (43°±1°), indicative of densely packed ODS monolayers.<sup>14</sup> These considerations rule out any significant contribution of monolayer disorder on the observed time-dependent SHG. The residual time dependence is unlikely to come from ambient-gas-assisted trapping, but may reveal the contribution of trapping at the semiconductor/oxide interface or in the bulk oxide.

The significant variations in TD-SHG behavior between samples that differ ostensibly only in their surface terminations suggests that the limiting factor is not sample heating

or strain at the Si/SiO<sub>2</sub> interface. Indeed, one of the advantages of the high-repetition rate, ultrashort-pulse lasers used in our experiments is that measurable SH signals can be obtained using pulse fluences that induce minimal heating effects compared to effects of charge transfer in the sample.<sup>2</sup> We estimate that the heating induced per single pulse is on the order of 0.08 K and that the steady-state temperature rise attained by cumulative pulse heating to be 2 K.<sup>2</sup> When the finite size of the sample is considered the temperature rise can be on the order of 14 K, which is also negligible.<sup>2</sup> The influence of strain at the Si–SiO<sub>2</sub> interface on TD SHG can be ruled out based on the fact that the monolayer formation leaves the oxide intact.

#### IV. SUMMARY AND CONCLUSIONS

TD-SHG probes, in real time, laser-induced charge trapping at semiconductor interfaces. Utilizing chemical modification of the interface it is possible to turn on and turn off different contributions to the charge trapping. The results of our experiments provide evidence that charge trapping at semiconductor interfaces involves charge trapping at oxide/ambient interface. These results highlight the major role played by the oxide layer and traps at the oxide–ambient interface. It appears that alternative passivating layers such as those provided by SAMs offer significant advantages, especially with regard to the elimination of charge trapping and associated phenomena.

#### ACKNOWLEDGMENTS

The authors acknowledge the support of the National Science Foundation, Grant No. CHE-9734273. Acknowledgment is made to the donors of the Petroleum Research Fund, administered by the ACS, for partial support of this research. The courtesy of Professor Chapman for the use of the ellipsometer and contact angle apparatus for sample characterization is appreciated.

- <sup>1</sup>J. G. Mihaychuk, J. Bloch, Y. Liu, and H. M. van Driel, *Opt. Lett.* **20**, 2063 (1995).
- <sup>2</sup>J. I. Dadap, X. F. Hu, N. M. Russell, J. G. Ekerdt, J. K. Lowell, and M. C. Downer, *IEEE J. Sel. Top. Quantum Electron.* **1**, 1145 (1995).
- <sup>3</sup>J. Bloch, J. G. Mihaychuk, and H. M. van Driel, *Phys. Rev. Lett.* **77**, 920 (1996).
- <sup>4</sup>J. G. Mihaychuk, N. Shamir, and H. M. van Driel, *Phys. Rev. B* **59**, 2164 (1999).
- <sup>5</sup>N. Shamir, J. G. Mihaychuk, H. M. van Driel, and H. J. Kreuzer, *Phys. Rev. Lett.* **82**, 359 (1999).
- <sup>6</sup>W. Wang *et al.*, *Phys. Rev. Lett.* **81**, 4224 (1998).
- <sup>7</sup>N. Shamir, J. G. Mihaychuk, and H. M. van Driel, *J. Appl. Phys.* **88**, 896 (2000).
- <sup>8</sup>N. Shamir, J. G. Mihaychuk, and H. M. van Driel, *J. Appl. Phys.* **88**, 909 (2000).
- <sup>9</sup>A. Ulman, *Introduction to Ultrathin Organic Films: From Langmuir-Blodgett to Self-Assembly* (Academic, San Diego, CA, 1991).
- <sup>10</sup>C. Boulas, J. V. Davidovits, F. Rondelez, and D. Vuillaume, *Phys. Rev. Lett.* **76**, 4797 (1996).
- <sup>11</sup>D. Vuillaume, C. Boulas, J. Collet, J. V. Davidovits, and F. Rondelez, *Appl. Phys. Lett.* **69**, 1646 (1996).
- <sup>12</sup>G. Lüpke, *Surf. Sci. Rep.* **35**, 75 (1999).
- <sup>13</sup>E. D. Palik, *Handbook of Optical Constants of Solids*, Part I (Academic, San Diego, CA, 1998).
- <sup>14</sup>A. Y. Fadeev and T. J. McCarthy, *Langmuir* **16**, 7268 (2000).
- <sup>15</sup>T. Ye, D. Wynn, R. Dudek, and E. Borguet, *Langmuir* **17**, 4497 (2001).
- <sup>16</sup>J. Sagiv, *J. Am. Chem. Soc.* **102**, 92 (1980).
- <sup>17</sup>D. L. Allara, A. N. Parikh, and F. Rondelez, *Langmuir* **11**, 2357 (1995).
- <sup>18</sup>J. B. Brzoska, I. Benazouz, and F. Rondelez, *Langmuir* **10**, 4367 (1994).
- <sup>19</sup>R. W. P. Fairbank and M. J. Wirth, *J. Chromatogr., A* **830**, 285 (1999).
- <sup>20</sup>S. R. Wasserman, Y. T. Tao, and G. M. Whitesides, *Langmuir* **5**, 1074 (1989).
- <sup>21</sup>R. Williams, *Phys. Rev.* **140**, A569 (1965).
- <sup>22</sup>P. Lautenschlager, M. Garriga, L. Vina, and M. Cardona, *Phys. Rev. B* **36**, 4821 (1987).
- <sup>23</sup>V. Fomenko, J. F. Lami, and E. Borguet, *Phys. Rev. B* **63**, 121316 (2001).
- <sup>24</sup>*The Si-SiO<sub>2</sub> System* edited by P. Balk (Elsevier, Amsterdam, 1988), Vol. 32.
- <sup>25</sup>R. W. Kempf, P. T. Wilson, J. D. Canterbury, E. D. Mishina, O. A. Aktsipetrov, and M. C. Downer, *Appl. Phys. B: Lasers Opt.* **68**, 325 (1999).
- <sup>26</sup>O. A. Aktsipetrov, A. A. Fedyanin, V. N. Golovkina, and T. V. Murzina, *Opt. Lett.* **19**, 1450 (1994).
- <sup>27</sup>J. I. Dadap, P. T. Wilson, M. H. Anderson, and M. C. Downer, *Opt. Lett.* **22**, 901 (1997).
- <sup>28</sup>D. H. Flinn, D. A. Guzonas, and R.-H. Yoon, *Colloids Surf., A* **87**, 163 (1994).
- <sup>29</sup>A. N. Parikh, D. L. Allara, I. B. Azouz, and F. Rondelez, *J. Phys. Chem.* **98**, 7577 (1994).
- <sup>30</sup>D. L. Angst and G. W. Simmons, *Langmuir* **7**, 2236 (1991).